

Polycomb repressive complex 2 attenuates ABA-induced senescence in Arabidopsis

Chunmei Liu^{1, 2, 3}, Jingfei Cheng^{1, 2, 3}, Yili Zhuang^{1, 2}, Luhuan Ye^{1, 2}, Zijuan Li^{1, 2}, Yuejun Wang^{1, 2}, Meifang Qi^{1, 2}, Yijing Zhang^{1, 2, *}

¹ National Laboratory of Plant Molecular Genetics, CAS Center for Excellence in Molecular Plant Sciences, Institute of Plant Physiology and Ecology, Shanghai Institutes for Biological Sciences, Chinese Academy of Sciences, Shanghai, 200032, China

² University of the Chinese Academy of Sciences, Beijing, 100049, China

³ Authors contributed equally to this work.

* **Correspondence:** Yijing Zhang (zhangyijing@sibs.ac.cn)

Tel. +86-21-54924206; Fax. +86-21-54924015

Running head: PRC2 attenuates ABA-induced senescence

Keywords: Polycomb repressive complex 2 (PRC2); H3K27 methyltransferase; CURLY LEAF (CLF); SWINGER (SWN); ABA; senescence

This article has been accepted for publication and undergone full peer review but has not been through the copyediting, typesetting, pagination and proofreading process, which may lead to differences between this version and the Version of Record. Please cite this article as doi: 10.1111/tpj.14125

This article is protected by copyright. All rights reserved.

Abstract

The phytohormone abscisic acid (ABA)-induced leaf senescence facilitates nutrient reuse and potentially contributes to enhancing plant stress tolerance. However, excessive senescence causes serious reductions in crop yield, and the mechanism by which senescence is finely tuned at different levels is still insufficiently understood. Here, we found that the double mutant of core enzymes of the Polycomb repressive complex 2 (PRC2) is hypersensitive to ABA in *Arabidopsis thaliana*. To elucidate the interplay between ABA and senescence at the genome level, we extensively profiled the transcriptomic and epigenomic changes triggered by ABA. We observed that H3K27me3 preferentially targets ABA-induced senescence-associated genes (SAGs). In the double, but not single, mutant of PRC2 enzymes, these SAGs were de-repressed and could be more highly induced by ABA compared with the wild-type, suggesting a redundant role for the PRC2 enzymes in negatively regulating ABA-induced senescence. Contrary to the rapid transcriptomic changes triggered by ABA, the reduction of H3K27me3 at these SAGs falls far behind the induction of their expression, indicating that PRC2-mediated H3K27me3 contributed to long-term damping of ABA-induced senescence to prevent an over-sensitive response. The findings of this study may serve as a paradigm for a global understanding of the interplay between the rapid effects of a phytohormone such as ABA and the long-term effects of the epigenetic machinery in regulating plant senescence processes and environmental responses.

Introduction

The phytohormone abscisic acid (ABA) is essential for optimizing plant water use during development and abiotic stress responses. ABA-induced leaf senescence allows for nutrient re-allocation and promotes drought tolerance (Rivero *et al.*, 2007, Zhao *et al.*, 2016). Transcriptional regulation is one major component of ABA signaling. Upon external stimuli, ABA is rapidly synthesized, further perceived by ABA receptors, and finally activates cascades of transcription factors (TFs) (Cutler *et al.*, 2010, Yoshida *et al.*, 2014). A recent high-throughput study based on chromatin immunoprecipitation followed by sequencing (ChIP-Seq) revealed that ABA signaling regulates the expression of thousands of genes via the chromatin binding of

ABA-related TFs at tens of thousands of loci (Song *et al.*, 2016). ABA response elements (ABREs) are the most common class of regulatory sequence enriched surrounding these TF binding loci that generally confer ABA inducibility of target genes (Cutler *et al.*, 2010, Yoshida *et al.*, 2014).

Intriguingly, ABA-responsive elements and genes were often found to be marked by H3K27me3 mediated by polycomb repressive complex 2 (PRC2) (Bouyer *et al.*, 2011, Lafos *et al.*, 2011, Wang *et al.*, 2016, Xiao *et al.*, 2017), indicating an active interplay between the stress hormone and the epigenetic machinery. PRC2 and PRC1 are the major families of Polycomb group (PcG) factors and generally act in concert to promote an inactive chromatin state. CURLY LEAF (CLF) and SWINGER (SWN) are catalytic subunits of PRC2 responsible for histone H3 lysine-27 tri-methylation. LIKE HETEROCHROMATIN PROTEIN 1 (LHP1, also named TERMINAL FLOWER 2; TFL2), the counterpart of the human Pc component, plays roles in both the PRC2 and PRC1 complexes (Turck *et al.*, 2007; Zhang *et al.*, 2007). While PRC2 is known to play an essential role in plant development (Schubert *et al.*, 2005, Derkacheva and Hennig, 2014, Grossniklaus and Paro, 2014, Mozgova and Hennig, 2015), the role of this complex in response to ABA and ABA-related stresses is incompletely understood (Kwon *et al.*, 2009, Sani *et al.*, 2013, Kleinmanns and Schubert, 2014, Liu *et al.*, 2014a, Liu *et al.*, 2014b, Avramova, 2015, Sanchez *et al.*, 2015). Previous work focusing on the relationship between PRC2 and abiotic stresses revealed that H3K27me3 occupied the promoters of major drought, salt, and cold response genes (Kwon *et al.*, 2009, Sani *et al.*, 2013, Liu *et al.*, 2014a, Liu *et al.*, 2014b), indicating that PRC2 actively participated in regulating stress responses. However, there was no consensus pattern of H3K27me3 change following stress treatment, and stress-induced gene expression was not always accompanied by the elimination of H3K27me3 in surrounding regions (Kwon *et al.*, 2009, Sani *et al.*, 2013, Liu *et al.*, 2014a, Liu *et al.*, 2014b). Mutation of the H3K27me3 enzyme *CLF* was associated with either increased or decreased expression of stress-induced genes (Liu *et al.*, 2014b). This issue is likely to be complicated by the fact that both ABA-dependent and ABA-independent pathways are activated by external stresses, obscuring the role of PcGs in the mixed signaling pathways. Thus, elucidating the role of PcGs in modulating ABA signaling is the key to clarifying their role in stress response.

A number of challenges are associated with characterizing the role of PRC2 in ABA response. First, both PRC2 and the ABA signaling pathway influence the transcription of thousands of genes; it is difficult to characterize the dynamic and quantitative epigenomic and transcriptomic changes among such a large number of genes with high confidence, thereby limiting an extensive understanding of the interplay between these two factors. Second, partially redundant roles were observed for the major H3K27me3 enzymes CLF and SWN(Chanvivattana *et al.*, 2004, Makarevich *et al.*, 2006). Previous analyses revealed that ABA-responsive elements are enriched for H3K27me3 loci redundantly controlled by H3K27 tri-methyltransferases CLF and SWN(Wang *et al.*, 2016) and more genetic evidence is required to pinpoint the role of the different PcG proteins.

The present study focused on the role of PRC2 enzymes in the ABA response. With the integration of genetic evidence and quantitative comparison of transcriptomic and epigenomic data, we observed that the *CLF* and *SWN* double mutant was hypersensitive to ABA and further revealed that CLF and SWN redundantly buffered ABA-induced expression of senescence-associated genes (SAGs). Upon ABA treatment, the H3K27me3 level in surrounding SAGs gradually decreased but lagged significantly behind ABA-induced transcription. The convergence of the rapid effects of ABA and the long-term damping effects of PRC2 on the regulation of plant senescence allows for both prompt and moderate responses to external stimuli.

Results

H3K27me3 targets a large proportion of ABA-responsive elements

Previous reports revealed that G-box ABREs are enriched for H3K27me3 loci redundantly controlled by the H3K27 trimethyltransferases CLF and SWN(Wang *et al.*, 2016). Here, we plotted the average H3K27me3 ChIP-Seq read density surrounding genome-wide ABREs and observed significant enrichment of H3K27me3 (Figure 1a; Table S1a). We next grouped H3K27me3 loci based on ChIP-Seq read density and plotted the percentage of regions with ABREs for each group. We found

that the higher the H3K27me3 level, the greater the percentage of loci with an ABRE (Figure 1b; Table S1b). The genomic tracks in Figure 1c illustrated the enrichment of H3K27me3 surrounding ABA-response genes. Together, these results indicate a close relationship between the ABA response and PcG-mediated H3K27me3.

The *clf-50 swn-1* double mutant is hypersensitive to ABA

To explore the role of PRC2 components in plant responses to ABA, we treated the mutants of major PRC2 members with exogenous ABA (Figure 2a and Figure S1), including the core enzymes *CLF*, *SWN*, and *LHP1* (Table S2a). The growth of the *clf-50 swn-1* double mutant and the *LHP1* mutants *lhp1-6* and *tfl2-2* was slowed with or without ABA treatment. Among these lines, the *clf-50 swn-1* double mutant was the most hypersensitive to ABA (Figure 2a); no obvious differences were observed for the single-gene mutants and *LHP1* mutants compared with the wild-type (WT) plants 8 d after ABA treatment (Figure 2a and Figure S1).

We next examined whether the hypersensitivity of *clf-50 swn-1* was associated with aberrant expression of 1,036 previously identified ABA-induced genes (Weng *et al.*, 2016). A large proportion of the ABA-induced genes were upregulated in the *clf-50 swn-1* double mutant; a much smaller number of these genes were upregulated in the *CLF* or *SWN* single mutants (Figure 2b; Table S2b), indicating that *CLF* and *SWN* redundantly repress transcription of these ABA-responsive genes directly or indirectly. Further functional enrichment analyses revealed that organ senescence was the most enriched gene ontology (GO) term for ABA-induced genes that were more highly expressed in *clf-50 swn-1* than in WT plants (Figure 2c and Table S2c). The genomic tracks shown in Figure 2d illustrate the higher expression of ABA-induced genes in *clf-50 swn-1*. Together, these results indicate that ABA-induced SAGs are likely to be kept in an inactive state by PRC2 under normal conditions.

The SAGs targeted by H3K27me3 are more highly induced by ABA in *clf-50 swn-1* compared with the wild-type

Given that CLF and SWN are the major H3K27 tri-methyltransferases, we hypothesized that H3K27me3 contributes to the suppression of ABA-induced gene expression. As expected, 54% of ABA-induced genes were directly marked by H3K27me3, significantly more than the proportion expected by chance (Figure 3a and Table S3a). Comparison of the enriched GO terms between H3K27me3 targets and ABA-induced genes revealed that leaf senescence was the top enriched term for H3K27me3 target genes inducible by ABA (Figure 3b and Table S3b). Notably, neither the gene set only induced by ABA nor the gene set only targeted by H3K27me3 was enriched for leaf senescence, indicating that ABA-induced senescence is potentially modulated by H3K27me3 (Figure 3b and Table S3c-d). Accordingly, we collected 3,292 *Arabidopsis thaliana* SAGs defined previously through microarray data (see Experimental Procedures for further description)(Breeze *et al.*, 2011) and found 772 SAGs that were targeted by H3K27me3. We further examined their expression levels in *clf-50 swn-1* and WT plants with or without ABA treatment for 5 h or 4 d (Figure 3c-d and Table S4). Compared with WT, these genes were generally upregulated in *clf-50 swn-1* plants under normal conditions and were further induced to a higher extent in the double mutant following ABA treatment than in the WT). Notably, in WT plants, there was a dramatic induction of SAGs after 5 h ABA treatment; after 4 d ABA treatment, however, the global expression pattern displayed no further changes. A similar pattern was obtained from public RNA-Seq data sets characterizing the dynamic transcriptomic changes triggered by ABA (Song *et al.*, 2016) (Figure S2). This pattern has been mainly attributed to a negative feedback regulatory loop that gated acute ABA responses (Cutler *et al.*, 2010). Here, we revealed that mutation of the PRC2 enzymes leads to a constant increase in ABA-induced SAG expression, indicating that in addition to the feedback loop, the epigenomic modification is another layer of control limiting ABA-induced SAG expression. Given that ABA is rapidly accumulated in unfavorable conditions, damping of ABA-induced senescence by PRC2 may help to avoid over-sensitivity in dynamic environments.

H3K27me3 changes follow the induction of gene expression and TF binding triggered by ABA

We then profiled H3K27me3 changes and transcriptomic changes of the 772 H3K27me3-targeted SAGs triggered by ABA and investigated how H3K27me3 contributed to the damping of ABA-induced SAG expression induction. Both H3K27me3 ChIP-Seq and RNA-seq were performed using Arabidopsis seedlings with and without ABA treatment for 5 h and for 4 d, followed by quantification of H3K27me3 changes using DEseq package (Anders and Huber, 2010) (see Methods; statistics in Table S5). The 5 h ABA treatment triggered similar expression changes as the 3 h ABA treatment (Figure S3). The expression of *CLF* and *SWN* did not change significantly following ABA treatment. After 5 h ABA treatment, none of the 772 H3K27me3-targeted SAGs displayed significant changes in H3K27me3 level (Figure 4a and Figure S4a). After 4 d ABA treatment, only 13 genes were found to have a significant, but weak, reduction in H3K27me3 level; (Figure 4b). The pattern and extent of H3K27me3 changes were similar following 50 μ M (Figure 4b) and 100 μ M ABA treatment (Figure S4b). Conversely, among the 772 SAGs, 134 were upregulated and 6 were downregulated shortly after ABA treatment (Figure 4c and Figure S4c). Thus, the ABA-triggered expression changes were considerably more rapid and extensive than the H3K27me3 changes.

If PRC2-mediated H3K27me3 functions to limit transcription of SAGs, it is natural to expect that the gradual reduction of H3K27me3 contributed to slow increases in target gene expression. We thus examined changes in the expression of the 13 SAGs with reduced H3K27me3 triggered by ABA, as well as the remaining 759 SAGs with no significant H3K27me3 change (Figure 4d-e and Figure S4d-e). As expected, after 4 d ABA treatment, the expression of the 13 SAGs obviously increased while no apparent expression change was found for the 759 SAGs with no H3K27me3 change. Thus, the slow change of H3K27me3 contributes to the attenuation of ABA-induced expression of SAGs.

Given that a gradual decrease in H3K27me3 levels is responsible for extending the expression of ABA-responsive genes, which factor(s) mediate the rapid response triggered by ABA? Given that a number of well-established TFs are involved in ABA signaling, we examined the previously published binding profiles of ABA-related TFs

that increase 4 h of ABA treatment (Song *et al.*, 2016). Binding of 21 ABA-related TFs was significantly enriched in ABA-induced genes whether or not they were covered by H3K27me3 (Figure 4f and Figure S5). Genomic tracks in Figure 4G illustrate the rapid binding of ABF1 and gradual decrease in H3K27me3 surrounding ABA-induced SAGs. Together, the binding of ABA-related TFs is responsible for the rapid induction of ABA-induced genes and the persistence of H3K27me3 potentially contributes to damping of ABA-induced SAGs (Figure 5).

Discussion

While it has been well established that H3K27me3 is present in the regions surrounding major stress-response genes, the relationship between stress-triggered changes in transcription and the H3K27me3 level remains unclear and the role of PRC2 enzymes in this process is not yet fully understood (Kwon *et al.*, 2009, Sani *et al.*, 2013, Kleinmanns and Schubert, 2014, Liu *et al.*, 2014a, Liu *et al.*, 2014b, Avramova, 2015, Sanchez *et al.*, 2015). H3K27me3 levels in regions surrounding six dehydration-induced genes did not change under stress conditions (Liu *et al.*, 2014b) and it was proposed that, unlike the active role of H3K27me3 in regulating differentiation and development, transcription of stress response genes may be limited, but not blocked, by H3K27me3 (Avramova, 2015). However, genome-wide studies have revealed that following salt treatment, loci with decreased H3K27me3 modification were associated with similar proportions of increased and decreased genes (Sani *et al.*, 2013). Additionally, while the *CLF* mutant was more sensitive to dehydration, half of the six stress response genes were upregulated and half were repressed in the *CLF* mutant (Liu *et al.*, 2014b). Thus, this hypothesis needs further verification using a combination of additional genetic evidence and high-throughput analysis. In the present study, genetic evidence and quantitative integration of transcriptomic and epigenomic data were used to reveal that the *CLF* and *SWN* double mutant was hypersensitive to ABA; the single mutants were not hypersensitive, indicating a redundant role for CLF and SWN in repressing ABA-induced responses (Figure 2a). This is further supported by the following lines of evidence. First, our previous analyses revealed that ABA-responsive elements were significantly enriched for H3K27me3 marks redundantly controlled by CLF and

SWN(Wang *et al.*, 2016). Second, the top enriched GO terms for genes commonly regulated by CLF and SWN include responses to ABA and water deprivation (Figure S6). Third, the ABA-induced SAGs were preferentially upregulated in the *CLF* and *SWN* double mutant but not in single-gene mutants (Figure 2b-C). Thus, the redundant role of CLF and SWN in repressing ABA-induced SAGs is supported at both the phenotypic and molecular levels.

Given that ABA signaling is the major pathway triggered by environmental stresses, we examined the H3K27me3 binding profiles around genes responsive to typical abiotic stimuli. Specifically, genes whose expression was affected by drought, cold, and salt were collected and were further partitioned into three groups based on expression change patterns. Group I contained genes strongly upregulated by these stresses while group II contained genes that were mildly induced by some of the stresses (Figure S7a; Table S6). Group III contained genes commonly repressed by these stresses. In group I, 52% of genes were induced after 3 h ABA treatment while only 0.3% of the group II genes were induced at this time (Figure S7b; Table S6). H3K27me3 covered 30% of the genes in group I with 59% of these H3K27me3 targets being SAGs; this was a significantly higher proportion than that expected by chance. Group II and III were not enriched for H3K27me3 targets or SAGs (Figure S7c; Table S6). Taken together, genes commonly induced by these abiotic stresses tend to be regulated by both ABA and PRC2; elucidating the role of PRC2 in modulating ABA signaling is the key to investigating its role in stress responses.

In addition to H3K27me3, H3K4me3 and histone acetylations are major epigenetic modifications actively involved in regulating gene activity. Despite that some of these modifications were reported to be involved in ABA or stress responses (Sridha and Wu, 2006), their changes are prompt and extensive. For example, Liu *et al.*, 2014b reported a rapid increase in H3K4me3 that was highly correlated with target transcription activity 90 min after a dehydration treatment; this was independent of the H3K27me3 level. Consistently, in another study in Arabidopsis, the changes in both H3K4me3 and H3K9K14ac were positively correlated with target expression changes 3 h after ABA treatment(Chen *et al.*, 2010). We performed H3K27ac ChIP-qPCR with nine H3K27me3-targeted SAGs and observed rapid increases in the H3K27ac level 5 h after ABA treatment (Figure S8). Thus, among

these histone modifications regulating gene activity, H3K27me3 is the major mark displayed long-term effects on the attenuation of ABA responses.

One interesting issue that needs to be addressed further is the mechanism underlying the specific release of H3K27me3 surrounding ABA-induced genes. The binding of ABA-related TFs is likely to play a major role in this process. It was reported that the ABA-responsive factor Nuclear Factor Y subunit B2 (NFYB2) could recruit H3K27me3 de-methyltransferase (Hou *et al.*, 2014). We, therefore, processed recently published ChIP-Seq data of 21 ABA-responsive TFs (Song *et al.*, 2016) and calculated the quantitative changes in their binding after 4 h ABA treatment (Table S7). The binding of these TFs commonly increased in a subset of their target loci (Figure S9a). We further examined the H3K27me3 change pattern surrounding these loci in response to ABA. After 4 d ABA treatment, regions commonly bound by these TFs tended to have a reduction in H3K27me3 (Figure S9; Table S7). In addition, given that genes with strong ABA-induced H3K27ac displayed significant H3K27me3 reduction after 4 d ABA treatment (Figure S8), H3K27ac may also be responsible for the progressive decrease in H3K27me3.

Whether PRC2-mediated H3K27me3 also participates in attenuating developmentally programmed (age-associated) senescence is another interesting issue. A recent report in human cells demonstrated a progressive loss of H3K27me3 marks and transcriptional activation of SAGs, with this gradual decrease in H3K27me3 dependent on the enzymatic activity of EZH2 (Ito *et al.*, 2018). Furthermore, induction of senescence by reduction of EZH2 occurs before the reduction of H3K27me3, thus suggesting the second mechanism by which depletion of EZH2 rapidly initiates a DNA damage response prior to a reduction in the level of H3K27me3 marks. We examined the expression of *CLF* and *SWN* during aging using previously published microarray data (Breeze *et al.*, 2011) and observed a significant reduction in *CLF* but not *SWN* expression. We further performed H3K27me3 ChIP-qPCR in old and young leaves using the promoters of several SAGs and observed a weak reduction in H3K27me3 level in old leaves (Figure S10). Thus, PRC2 may also participate in age-associated senescence, though further genetic and genome-wide evidence is required to confirm this. Additionally, further investigation is also required to determine whether there is also a second mechanism by which PRC2 enzymes induce senescence independent of H3K27me3 in plants.

In summary, the present study focused on the effect of PRC2 on plant ABA responses, the major pathway triggered by most abiotic stresses. We discovered redundant roles for the core PRC2 enzymes in damping ABA-induced senescence. The convergence of the rapid effects of ABA and the long-term effects of PRC2 in controlling plant senescence ensures responses to environmental cues are both prompt and moderate.

Experimental Procedures

Plant materials and growth conditions

Arabidopsis seedlings were grown on 1/2 Murashige and Skoog (MS) medium without sucrose (2% agar, PH 5.8) under LD conditions. The mutants *clf-50*, *swn-1*, and *clf-50 swn-1* were in the *Ws* background(Chanvivattana *et al.*, 2004). The mutants *clf-29* (SALK_N521003)(Bouveret *et al.*, 2006), *swn-21* (He *et al.*, 2012), *lhp1-6* (SALK_011762) (Exner *et al.*, 2009), and *tf12-2* (CS3797)(Larsson *et al.*, 1998) were in the Columbia (Col-0) background. All are null or strong mutants except *swn-1*, which is a hypomorphic allele (Table S2a). For ABA treatment, ten-day-old seedlings were transferred onto 1/2 MS medium containing 50 μ M ABA or 100 μ M ABA. After both 5 h and 4 d treatment, the aerial parts were harvested and either frozen in liquid nitrogen for RNA isolation or directly vacuum-infiltrated with formaldehyde crosslinking solution for use in the ChIP assay.

ChIP-seq and RNA-seq sample preparation

All ChIP samples were prepared in biological duplicates. The ChIP assay was performed with the antibody against H3 trimethyl-Lys 27 (Upstate, USA, Cat. 07-449) and H3 acetyl-Lys 27 (Upstate, USA, Cat. 07-360) as previously described(Wang *et al.*, 2016). More than 10 ng of ChIP DNA or 2 μ g of total RNA from each sample was used for Illumina library generation according to the manufacturer's instructions (Illumina, <http://www.illumina.com/>). Library construction and deep sequencing were performed by Genergy Biotechnology Co. Ltd. (Shanghai, China) using Illumina HiSeq 2500 following the manufacturer's instructions (Illumina). Raw data comprised 150 bp of pair-end sequences for ChIP-seq and RNA-seq. Primers for H3K27ac and H3K27me3 qPCR analysis are listed in Table S8.

ChIP-seq and RNA-seq data analysis

The sequencing reads were first cleaned by removing bases with low-quality scores (<20) and irregular GC content, cutting sequencing adaptors, and subsequent filtering of short reads. The cleaned reads were mapped to the Arabidopsis genome (TAIR10) using BWA 0.7.5a-r405 (Li and Durbin, 2009) for DNA sequencing and TOPHAT v2.0.8 (Kim *et al.*, 2013a) for RNA sequencing, both with default settings. Uniquely mapped reads with MAPQ>20 were collected for further analysis (detailed statistics in Table S9).

For ChIP-seq data analysis, SICER_V1.1 (Zang *et al.*, 2009) was used to identify read-enriched regions (peaks) for H3K27me3 ChIP-seq data. MACS1.4 (Zhang *et al.*, 2008) was used to identify peaks for TF-binding ChIP-seq data. The target gene of each peak was defined as the gene that has a given peak(s) in the promoter region (1 kb up- or downstream of the transcription start site). DEseq (Anders and Huber, 2010) was applied to characterize the change in H3K27me3 level in genes triggered by ABA. ABA-regulated H3K27me3 regions were selected based on the following criteria: P -value <0.05 and $|\log_2(\text{fold-change of read density in target gene})| > 1$.

For RNA-seq data analysis, differentially expressed genes were detected by DESeq (Anders and Huber, 2010) based on the combined criteria: $|\log_2(\text{fold change})| > 1$ and P value < 0.05. To dissect the relationship between transcriptomic changes across samples, genes with differential expression in at least one comparison were collected and further partitioned via hierarchical clustering or k-means clustering in R version 3.3.3 (Team, 2013).

Integrative Genomics Viewer (IGV) was used to illustrate the genomic tracks (Thorvaldsdottir *et al.*, 2013); ChIP-seq and RNA-seq samples were normalized to the same sequencing depth. SAGs were defined in a previous study, i.e. genes in clusters 27–48 were described as being upregulated during leaf senescence (Breeze *et al.*, 2011).

Data availability

The H3K27me3 ChIP-seq and RNA-seq data generated in this study for plants treated with or without ABA (summarized in Table S9a) were deposited in the Gene Expression Omnibus (GEO <http://www.ncbi.nlm.nih.gov/geo/>) under the accession number GSE98301.

Sources for the public data used in this study are listed in Table S9b. Both RNA-seq data from the time-course of ABA treatment and ChIP-Seq data of ABA-related TFs are under accession number GSE80568 (Song *et al.*, 2016). RNA-Seq data of 3 h of 50 μ M ABA treatment are under accession number GSE65739 (Weng *et al.*, 2016). Microarray data of drought, salt, and cold treatments are under accession numbers GSE10670, GSE40061, GSE6583, GSE39236, GSE53308, GSE3326, and GSE43818 (Lee *et al.*, 2005, Catala *et al.*, 2007, Perera *et al.*, 2008, Guan *et al.*, 2013, Kim *et al.*, 2013b, Pandey *et al.*, 2013, Allu *et al.*, 2014).

Tracks for all sequencing data generated in this study and related public data can be visualized by JBrowse (Skinner *et al.*, 2009) using the following link: http://bioinfo.sibs.ac.cn/browser/tair10/pcg_aba.html. It is worth noting that the samples were treated, processed, and sequenced separately so it is normal to observe different signal-noise ratios; visualization using the genomic track normalized by the sequencing depth is not necessarily reliable. To make quantitative comparison across ChIP-seq datasets, we calculated the number of reads in the promoter (1 kb upstream of the transcriptional start site) and gene body region for each gene and applied DEseq to detect differential binding of H3K27me3 between samples treated or not treated with ABA. While the raw intensity is not directly comparable between replicates, the differential binding is highly similar between replicates (Figure 4 and Figure S4).

Acknowledgments

Y.Z. designed the study. C.L., Y. Z., L.Y., and Z.L. performed the experiments. J.C., Y.W., and M.Q. carried out the analysis. Y.Z. wrote the manuscript with input from all authors.

We thank Prof. Lin Xu for providing experimental conditions. Prof. Yang Zhao from the Shanghai Center for Stress Biology for valuable advice on physiological experiments. We thank Prof. Zhen Shao from the CAS-MPG Partner Institute for the thoughtful discussions.

This work was supported by grants from the National Natural Science Foundation of China (31570319, 31770285), Shanghai Pujiang Program (15PJ1409600), and sponsored by Shanghai Institutes for Biological Sciences, Chinese Academy of Sciences.

We thank Emma Tacken, PhD, from Liwen Bianji, Edanz Group China (www.liwenbianji.cn/ac), for editing the English text of a draft of this manuscript.

Conflict of Interest

The authors have no conflicts of interest to declare.

Legends for 10 supporting Figures

Supporting Figure S1. *CLF*, *SWN*, and *LHP1* mutants and wild-type (WT) plants grown without (a) or with (b) ABA treatment. For ABA treatment, plants were grown in 1/2 MS medium for 10 d followed by treatment with 50 μ M ABA for 8 d. Scale bar = 1 cm.

Supporting Figure S2. Dynamic transcriptomic changes of ABA-induced genes based on public RNA-seq datasets under GEO accession number GSE80565 (Song *et al.*, 2016). ABA-induced genes were defined as genes induced by ABA at any of the given time points.

Supporting Figure S3. Scatter plot showing the high correlation of expression change between 5 h ABA treatment (data generated in this study) and 3 h ABA treatment (Weng *et al.*, 2016).

Supporting Figure S4. Comparative analysis of the changes in H3K27me3 levels and gene expression after short- and long-term ABA treatment.

Supporting Figure S5. Average ABA-related TF ChIP-seq read density surrounding ABA-induced H3K27me3 targets (purple), H3K27me3 targets only (blue), and ABA-induced genes only (pink).

Supporting Figure S6. Responses to ABA and water deprivation are among the top enriched GO terms for genes commonly regulated by CLF and SWN.

Supporting Figure S7. A significant proportion of the genes commonly induced by abiotic stresses are regulated by both ABA and PRC2.

Supporting Figure S8. H3K27ac ChIP-qPCR at the promoters of SAGs.

Supporting Figure S9. Increased binding of ABA-related TFs is associated with reduced H3K27me3 levels following ABA treatment.

Supporting Figure S10. H3K27me3 ChIP-qPCR at the promoters of selected SAGs using old leaves (the first six rosette leaves) and young leaves (the last six rosette leaves) of 40-day-old seedlings. Primers are listed in Table S8b.

Legends for 9 Supporting Tables

Supporting Table S1. Relationship between the genomic location of ABREs and H3K27me3 peaks.

Supporting Table S2. Characterization of PRC2 mutants and transcriptomic changes in *CLF* and *SWN* mutants.

Supporting Table S3. Overlap between ABA-induced genes and H3K27me3 targets, as well as enriched functions.

Supporting Table S4. The expression levels of 772 H3K27me3-targeted SAGs in *clf-50 swn-1* and wild-type plants after 5 h and 4 d ABA treatments.

Supporting Table S5. Quantitative changes in H3K27me3 level in 772 SAGs triggered by short- and long-term ABA treatments.

Supporting Table S6. Enrichment of abiotic stress-induced genes in H3K27me3 targets and SAGs.

Supporting Table S7. Statistics of the quantitative changes of ABA-related TFs and H3K27me3 triggered by ABA.

Supporting Table S8. Primers for the H3K27ac (a) and H3K27me3 (b) ChIP-qPCR assay in Figure S8 and Figure S10.

Supporting Table S9. Summary of ChIP-seq and RNA-seq data generated in the present study (a) and from public databases (b).

References

- Allu, A.D., Soja, A.M., Wu, A.H., Szymanski, J. and Balazadeh, S.** (2014) Salt stress and senescence: identification of cross-talk regulatory components. *Journal of Experimental Botany*, **65**, 3993-4008.
- Anders, S. and Huber, W.** (2010) Differential expression analysis for sequence count data. *Genome Biol*, **11**, R106.
- Avramova, Z.** (2015) Transcriptional 'memory' of a stress: transient chromatin and memory (epigenetic) marks at stress-response genes. *Plant J*, **83**, 149-159.
- Bouveret, R., Schonrock, N., Gruissem, W. and Hennig, L.** (2006) Regulation of flowering time by Arabidopsis MSI1. *Development*, **133**, 1693-1702.
- Bouyer, D., Roudier, F., Heese, M., Andersen, E.D., Gey, D., Nowack, M.K., Goodrich, J., Renou, J.P., Grini, P.E., Colot, V. and Schnittger, A.** (2011) Polycomb repressive complex 2 controls the embryo-to-seedling phase transition. *PLoS Genet*, **7**, e1002014.
- Breeze, E., Harrison, E., McHattie, S., Hughes, L., Hickman, R., Hill, C., Kiddle, S., Kim, Y.S., Penfold, C.A., Jenkins, D., Zhang, C., Morris, K., Jenner, C., Jackson, S., Thomas, B., Tabrett, A., Legaie, R., Moore, J.D., Wild, D.L., Ott, S., Rand, D., Beynon, J., Denby, K., Mead, A. and Buchanan-Wollaston, V.** (2011) High-resolution temporal profiling of transcripts during Arabidopsis leaf senescence reveals a distinct chronology of processes and regulation. *Plant Cell*, **23**, 873-894.
- Catala, R., Ouyang, J., Abreu, I.A., Hu, Y., Seo, H., Zhang, X. and Chua, N.H.** (2007) The Arabidopsis E3 SUMO ligase SIZ1 regulates plant growth and drought responses. *Plant Cell*, **19**, 2952-2966.
- Chanvivattana, Y., Bishopp, A., Schubert, D., Stock, C., Moon, Y.H., Sung, Z.R. and Goodrich, J.** (2004) Interaction of Polycomb-group proteins controlling flowering in Arabidopsis. *Development*, **131**, 5263-5276.

- Chen, L.T., Luo, M., Wang, Y.Y. and Wu, K.Q.** (2010) Involvement of Arabidopsis histone deacetylase HDA6 in ABA and salt stress response. *Journal of Experimental Botany*, **61**, 3345-3353.
- Cutler, S.R., Rodriguez, P.L., Finkelstein, R.R. and Abrams, S.R.** (2010) Abscisic acid: emergence of a core signaling network. *Annu Rev Plant Biol*, **61**, 651-679.
- Derkacheva, M. and Hennig, L.** (2014) Variations on a theme: Polycomb group proteins in plants. *J Exp Bot*, **65**, 2769-2784.
- Exner, V., Aichinger, E., Shu, H., Wildhaber, T., Alfarano, P., Caflisch, A., Grisse, W., Kohler, C. and Hennig, L.** (2009) The Chromodomain of LIKE HETEROCHROMATIN PROTEIN 1 Is Essential for H3K27me3 Binding and Function during Arabidopsis Development. *Plos One*, **4**, e5335.
- Grossniklaus, U. and Paro, R.** (2014) Transcriptional Silencing by Polycomb-Group Proteins. *Csh Perspect Biol*, **6**, a019331.
- Guan, Q.M., Wu, J.M., Yue, X.L., Zhang, Y.Y. and Zhu, J.H.** (2013) A Nuclear Calcium-Sensing Pathway Is Critical for Gene Regulation and Salt Stress Tolerance in Arabidopsis. *Plos Genetics*, **9**, e1003755.
- He, C.S., Chen, X.F., Huang, H. and Xu, L.** (2012) Reprogramming of H3K27me3 Is Critical for Acquisition of Pluripotency from Cultured Arabidopsis Tissues. *Plos Genetics*, **8**, e1002911.
- Hou, X., Zhou, J., Liu, C., Liu, L., Shen, L. and Yu, H.** (2014) Nuclear factor Y-mediated H3K27me3 demethylation of the SOC1 locus orchestrates flowering responses of Arabidopsis. *Nat Commun*, **5**, 4601.
- Ito, T., Teo, Y.V., Evans, S.A., Neretti, N. and Sedivy, J.M.** (2018) Regulation of Cellular Senescence by Polycomb Chromatin Modifiers through Distinct DNA Damage- and Histone Methylation-Dependent Pathways. *Cell Rep*, **22**, 3480-3492.
- Kim, D., Pertea, G., Trapnell, C., Pimentel, H., Kelley, R. and Salzberg, S.L.** (2013a) TopHat2: accurate alignment of transcriptomes in the presence of insertions, deletions and gene fusions. *Genome Biol*, **14**, R36.
- Kim, Y., Park, S., Gilmour, S.J. and Thomashow, M.F.** (2013b) Roles of CAMTA transcription factors and salicylic acid in configuring the low-temperature transcriptome and freezing tolerance of Arabidopsis. *Plant J*, **75**, 364-376.

- Kleinmanns, J.A. and Schubert, D.** (2014) Polycomb and Trithorax group protein-mediated control of stress responses in plants. *Biol Chem*, **395**, 1291-1300.
- Kwon, C.S., Lee, D., Choi, G. and Chung, W.I.** (2009) Histone occupancy-dependent and -independent removal of H3K27 trimethylation at cold-responsive genes in Arabidopsis. *Plant J*, **60**, 112-121.
- Lafos, M., Kroll, P., Hohenstatt, M.L., Thorpe, F.L., Clarenz, O. and Schubert, D.** (2011) Dynamic regulation of H3K27 trimethylation during Arabidopsis differentiation. *PLoS Genet*, **7**, e1002040.
- Larsson, A.S., Landberg, K. and Meeks-Wagner, D.R.** (1998) The TERMINAL FLOWER2 (TFL2) gene controls the reproductive transition and meristem identity in Arabidopsis thaliana. *Genetics*, **149**, 597-605.
- Lee, B.H., Henderson, D.A. and Zhu, J.K.** (2005) The Arabidopsis cold-responsive transcriptome and its regulation by ICE1. *Plant Cell*, **17**, 3155-3175.
- Li, H. and Durbin, R.** (2009) Fast and accurate short read alignment with Burrows-Wheeler transform. *Bioinformatics*, **25**, 1754-1760.
- Liu, N., Ding, Y., Fromm, M. and Avramova, Z.** (2014a) Different gene-specific mechanisms determine the 'revised-response' memory transcription patterns of a subset of A. thaliana dehydration stress responding genes. *Nucleic Acids Res*, **42**, 5556-5566.
- Liu, N., Fromm, M. and Avramova, Z.** (2014b) H3K27me3 and H3K4me3 Chromatin Environment at Super-Induced Dehydration Stress Memory Genes of Arabidopsis thaliana. *Mol Plant*, **7**, 502-513.
- Makarevich, G., Leroy, O., Akinci, U., Schubert, D., Clarenz, O., Goodrich, J., Grossniklaus, U. and Kohler, C.** (2006) Different Polycomb group complexes regulate common target genes in Arabidopsis. *EMBO Rep*, **7**, 947-952.
- Mozgova, I. and Hennig, L.** (2015) The polycomb group protein regulatory network. *Annu Rev Plant Biol*, **66**, 269-296.
- Pandey, N., Ranjan, A., Pant, P., Tripathi, R.K., Ateek, F., Pandey, H.P., Patre, U.V. and Sawant, S.V.** (2013) CAMTA 1 regulates drought responses in Arabidopsis thaliana. *Bmc Genomics*, **14**, 216.
- Perera, I.Y., Hung, C.Y., Moore, C.D., Stevenson-Paulik, J. and Boss, W.F.** (2008) Transgenic Arabidopsis Plants Expressing the Type 1 Inositol 5-Phosphatase

Exhibit Increased Drought Tolerance and Altered Abscisic Acid Signaling. *Plant Cell*, **20**, 2876-2893.

- Rivero, R.M., Kojima, M., Gepstein, A., Sakakibara, H., Mittler, R., Gepstein, S. and Blumwald, E.** (2007) Delayed leaf senescence induces extreme drought tolerance in a flowering plant. *P Natl Acad Sci USA*, **104**, 19631-19636.
- Sanchez, M.D., Aceves-Garcia, P., Petrone, E., Steckenborn, S., Vega-Leon, R., Alvarez-Buylla, E.R., Garay-Arroyo, A. and Garcia-Ponce, B.** (2015) The impact of Polycomb group (PcG) and Trithorax group (TrxG) epigenetic factors in plant plasticity. *New Phytol*, **208**, 684-694.
- Sani, E., Herzyk, P., Perrella, G., Colot, V. and Amtmann, A.** (2013) Hyperosmotic priming of Arabidopsis seedlings establishes a long-term somatic memory accompanied by specific changes of the epigenome. *Genome Biol*, **14**, R59.
- Schubert, D., Clarenz, O. and Goodrich, J.** (2005) Epigenetic control of plant development by Polycomb-group proteins. *Current Opinion in Plant Biology*, **8**, 553-561.
- Shao, Z., Zhang, Y.J., Yuan, G.C., Orkin, S.H. and Waxman, D.J.** (2012) MAnorm: a robust model for quantitative comparison of ChIP-Seq data sets. *Genome Biology*, **13**.
- Skinner, M.E., Uzilov, A.V., Stein, L.D., Mungall, C.J. and Holmes, I.H.** (2009) JBrowse: A next-generation genome browser. *Genome Res*, **19**, 1630-1638.
- Song, L., Huang, S.C., Wise, A., Castanon, R., Nery, J.R., Chen, H., Watanabe, M., Thomas, J., Bar-Joseph, Z. and Ecker, J.R.** (2016) A transcription factor hierarchy defines an environmental stress response network. *Science*, **354**, aag1550.
- Sridha, S. and Wu, K.Q.** (2006) Identification of AtHD2C as a novel regulator of abscisic acid responses in Arabidopsis. *Plant J*, **46**, 124-133.
- Team, R.C.** (2013) R: A language and environment for statistical computing.
- Thorvaldsdottir, H., Robinson, J.T. and Mesirov, J.P.** (2013) Integrative Genomics Viewer (IGV): high-performance genomics data visualization and exploration. *Brief Bioinform*, **14**, 178-192.
- Wang, H., Liu, C., Cheng, J., Liu, J., Zhang, L., He, C., Shen, W.H., Jin, H., Xu, L. and Zhang, Y.** (2016) Arabidopsis Flower and Embryo Developmental Genes are Repressed in Seedlings by Different Combinations of Polycomb Group

Proteins in Association with Distinct Sets of Cis-regulatory Elements. *PLoS Genet*, **12**, e1005771.

Weng, J.K., Ye, M., Li, B. and Noel, J.P. (2016) Co-evolution of Hormone Metabolism and Signaling Networks Expands Plant Adaptive Plasticity. *Cell*, **166**, 881-893.

Xiao, J., Jin, R., Yu, X., Shen, M., Wagner, J.D., Pai, A., Song, C., Zhuang, M., Klasfeld, S., He, C., Santos, A.M., Helliwell, C., Pruneda-Paz, J.L., Kay, S.A., Lin, X., Cui, S., Garcia, M.F., Clarenz, O., Goodrich, J., Zhang, X., Austin, R.S., Bonasio, R. and Wagner, D. (2017) Cis and trans determinants of epigenetic silencing by Polycomb repressive complex 2 in Arabidopsis. *Nat Genet*, **49**, 1546-1552.

Yoshida, T., Mogami, J. and Yamaguchi-Shinozaki, K. (2014) ABA-dependent and ABA-independent signaling in response to osmotic stress in plants. *Curr Opin Plant Biol*, **21**, 133-139.

Zang, C., Schones, D.E., Zeng, C., Cui, K., Zhao, K. and Peng, W. (2009) A clustering approach for identification of enriched domains from histone modification ChIP-Seq data. *Bioinformatics*, **25**, 1952-1958.

Zhang, Y., Liu, T., Meyer, C.A., Eeckhoute, J., Johnson, D.S., Bernstein, B.E., Nusbaum, C., Myers, R.M., Brown, M., Li, W. and Liu, X.S. (2008) Model-based analysis of ChIP-Seq (MACS). *Genome Biol*, **9**, R137.

Zhao, Y., Chan, Z., Gao, J., Xing, L., Cao, M., Yu, C., Hu, Y., You, J., Shi, H., Zhu, Y., Gong, Y., Mu, Z., Wang, H., Deng, X., Wang, P., Bressan, R.A. and Zhu, J.K. (2016) ABA receptor PYL9 promotes drought resistance and leaf senescence. *Proc Natl Acad Sci U S A*, **113**, 1949-1954.

Legends for 5 Figures

Figure 1. H3K27me3 marks at ABA-responsive elements.

(a) Distribution of H3K27me3 ChIP-seq reads surrounding ABA-Response Elements (ABREs). H3K27me3 ChIP-seq data were previously generated (GSE67322). The X-axis represents the distance to ABREs. Y-axis represents the average H3K27me3 ChIP-seq read density of regions surrounding ABRE loci identified throughout the genome. (b) H3K27me3 loci with high read density tend to have ABREs. H3K27me3 peak regions were grouped by ChIP-seq read density. H3K27me3 ChIP-seq data were previously generated. Y-axis represents the percentage of peaks from each group containing ABREs. (c) Genomic tracks illustrate H3K27me3 ChIP-seq read density surrounding ABREs and ABA-response genes. H3K27me3 ChIP-seq data from a previous study and the present study showed a high correlation.

Figure 2. ABA induces accelerated senescence in the *clf-50 swn-1* double mutant.

(a) *CLF* and *SWN* mutants and wild-type (WT) plants were grown without (left panel) or with (right panel) ABA treatment. For ABA treatment, plants were grown in 1/2 MS medium for 10 d followed by treatment with 50 μ M ABA for 8 d. Scale bar = 1 cm. (b) Hierarchical clustering of the expression intensities of genes induced by ABA in WT and mutants of *CLF* and *SWN*. RNA-Seq data were generated in the present study (GSE98301). For each gene (represented by each row), z-score transformations were performed to normalize gene intensity across samples. Genes in the black box were preferentially expressed in *clf-50 swn-1*. Expression data are listed in Table S2b. (c) Top enriched GO terms for ABA-induced genes that were more highly expressed in *clf-50 swn-1* than in WT. Statistics are listed in Table S2c. (d) Genomic tracks illustrating expression intensity in WT and mutants of *CLF* and *SWN*; intensities are normalized by the number of total mapped reads. The first four tracks compared RNA-seq intensities between WT and mutants of *CLF* and *SWN* under normal conditions. The last 2 tracks compared WT plants treated with or without ABA. As ABA is resolved in ethanol, a similar amount of ethanol was added to the WT

(mock). RNA-seq data for the first 4 tracks were generated in the present study and public data (GSE65739) were used for the last 2 tracks.

Figure 3. A large proportion of ABA-induced SAGs are co-regulated by PRC2.

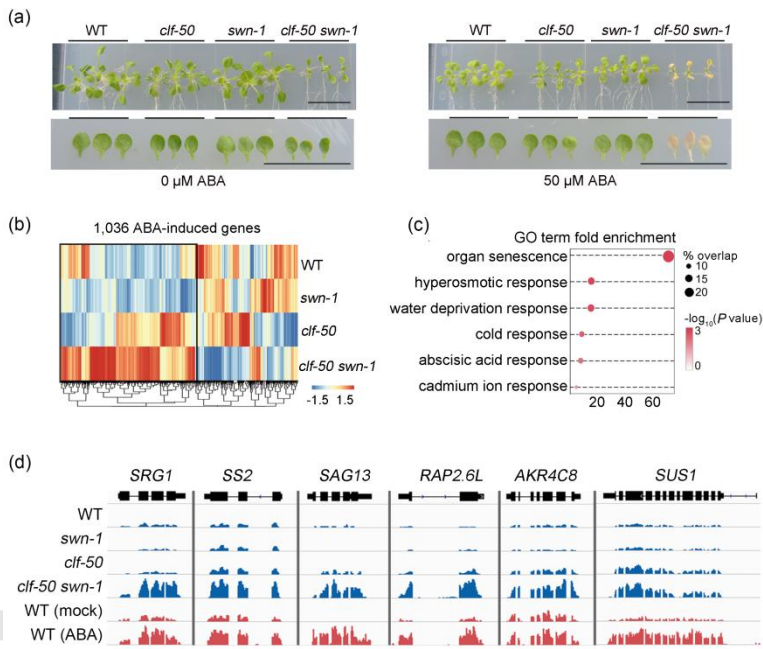
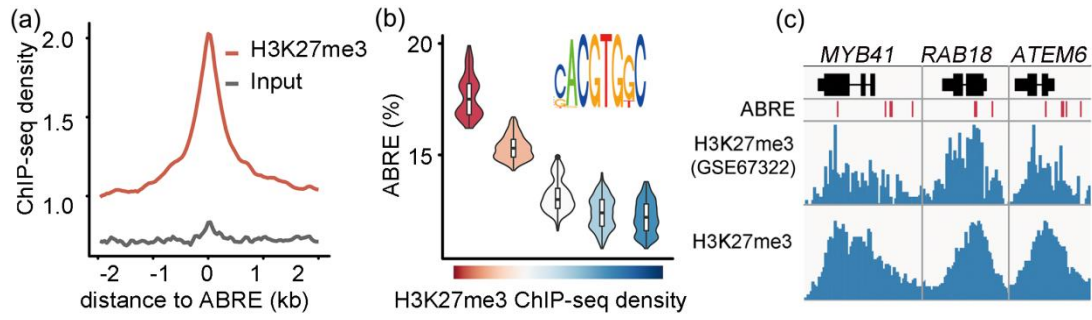
(a) Venn diagram showing the overlap between genes induced following 3 h of 50 μ M ABA treatment and H3K27me3 targets. The enrichment *P* value was calculated via Fisher's exact test. RNA-Seq data were from GSE65739. H3K27me3 ChIP-seq data were from the present study. See Table S3 for detailed information. (b) GO terms enriched in the overlapping genes between ABA-induced genes and H3K27me3 targets. The length of the bar represents the enrichment score. (c) Heatmap showing the expression of H3K27me3-targeted SAGs in the *clf-50 swn-1* double mutant and WT plants before and after ABA treatment. RNA-Seq data generated in the present study. (d) Genomic tracks illustrating that SAGs were more highly induced by ABA in *clf-50 swn-1* than in WT or single-gene mutants. RNA-Seq intensities were normalized by the number of total mapped reads. * indicates that the intensity was very high and the bar is truncated.

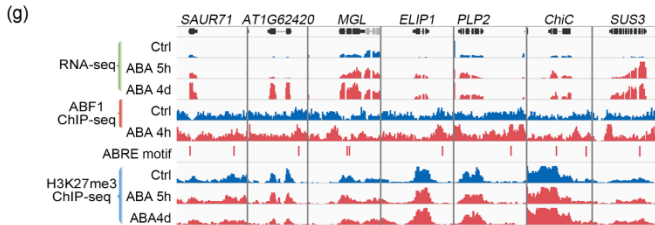
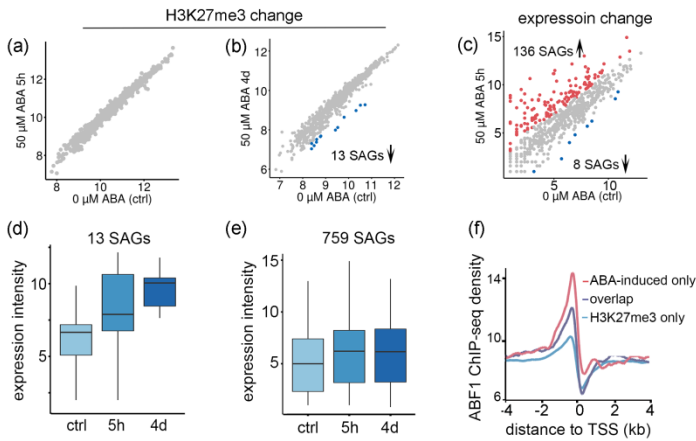
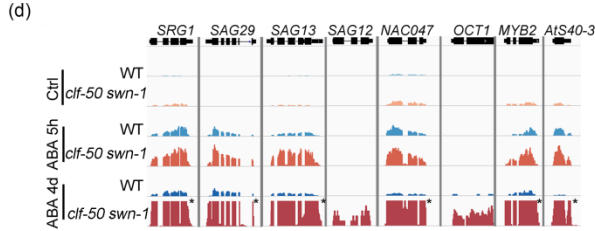
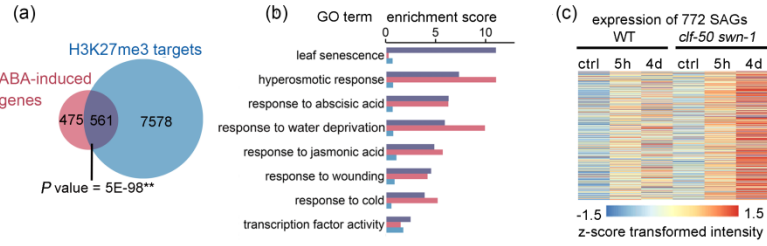
Figure 4. Comparative analysis of the changes in H3K27me3 levels, gene expression, and TF binding after short- and long-term ABA treatment.

(a-b) Scatter plot quantitatively comparing H3K27me3 level with or without 50 μ M ABA for 5 h (a) and 4 d (b). X and Y axes represent the DEseq-normalized H3K27me3 ChIP-seq read density in the promoter (1 kb upstream of the transcriptional start site) and gene body region. The numbers of SAGs with significant change of H3K27me3 level are marked. (c) Scatter plot comparing the expression changes with or without 5-h ABA treatment for the 772 SAGs. X and Y axes represent the DEseq-normalized RNA-Seq read density in \log_2 scale. The numbers of SAGs with significant expression change are marked. (d-e) Boxplot comparing the expression intensity of H3K27me3 targeted SAGs with (d) or without (e) H3K27me3 change following ABA treatment. Data for (A-E) were generated in the present study; detailed statistics are listed in Table S5. (f) ABF1 ChIP-Seq read density surrounding ABA-induced genes, H3K27me3 targets, and their overlapping genes. Similar plots

for 20 other ABA-related TFs are shown in Figure S5. These TF ChIP-seq data were generated previously (GSE80568). (g) Genomic tracks illustrate ABA-induced expression changes, ABF1 binding, and H3K27me3 changes surrounding SAGs.

Figure 5. Model illustrating the damping effect of PRC2-mediated H3K27me3 during the ABA response. In WT plants, ABA-induced SAGs are kept in an inactive state by H3K27me3 and are rapidly induced by ABA via ABA-related TFs accompanied by slow decreases in H3K27me3. The presence of H3K27me3 in the regions surrounding SAGs efficiently buffers further induction of these genes by ABA. In the *CLF* and *SWN* double mutant, these H3K27me3-marked SAGs are more highly expressed when compared with WT plants. When exposed to ABA, these SAGs are further induced to a much higher level without the damping effect of H3K27me3.





H3K27me3 buffers ABA-induced leaf senescence

